TR-1359

ELECTRONICALLY TUNABLE
MICROWAVE BANDPASS FILTER

Copy

by

Ting Hei Mak

Frank Reggia

October 1967

U.S. ARMY MATERIEL COMMAND

HARRY DIAMOND LABORATORIES

WASHINGTON, D.C. 20438

UNCLASSIFIED

Accession No._____   AD_____

Harry Diamond Laboratories, Washington, D. C. 20438

ELECTRONICALLY TUNABLE MICROWAVE BANDPASS FILTER
 Ting Hei Mak, Frank Reggia

TR-1359, October 1967, 36 pp text, 14 illus, DA-1C014501B31A
AMCMS Code: 5011.11.85400, HDL Proj. No. 28300, UNCLASSIFIED
Report

    An equivalent circuit of two orthogonal striplines coupled
by a ferrite (yttrium iron garnet) sphere is derived, using
the scattering matrix method. This derivation shows that a
nonreciprocal phase shifter can be represented by gyrator net-
works. Based on this analysis, a YIG bandpass filter, elec-
tronically tunable over a very broad frequency range (4:1),
is designed by coupling two broadband 180-deg phase shift
circuits with a small single crystal YIG sphere.

    This report also reviews some basic principles pertaining
to filter considerations, analyzes the filter circuit of two
orthogonal striplines coupled by a ferrite sphere, and
synthesizes the equivalent filter circuit by a scattering
matrix method. These results describe the operation of the
filter circuit under various terminal excitations.

UNCLASSIFIED

1. Ferrites
2. Magnetics
3. Microwaves
4. Bandpass
   filters

REMOVAL OF EACH CARD WILL BE NOTED ON INSIDE BACK COVER. AND REMOVED
CARDS WILL BE TREATED AS REQUIRED BY THEIR SECURITY CLASSIFICATION.

AD

TR-1359

ELECTRONICALLY TUNABLE

MICROWAVE BANDPASS FILTER

by

Ting Hei Mak
Frank Reggia

October 1967

U.S. ARMY MATERIEL COMMAND

HARRY DIAMOND LABORATORIES

WASHINGTON, D.C. 20438

1

CONTENTS

ILLUSTRATIONS

ABSTRACT

An equivalent circuit of two orthogonal striplines coupled by a ferrite (yttrium iron garnet) sphere is derived, using the scattering matrix method. This derivation shows that a non-reciprocal phase shifter can be represented by gyrator networks. Based on this analysis, a YIG bandpass filter, electronically tunable over a very broad frequency range (4:1), is designed by coupling two broadband 180-deg phase shift circuits with a small single crystal YIG sphere.

This report also reviews some basic principles pertaining to filter considerations, analyzes the filter circuit of two orthogonal striplines coupled by a ferrite sphere, and synthesizes the equivalent filter circuit by a scattering matrix method. These results describe the operation of the filter circuit under various terminal excitations.

1. INTRODUCTION

The phenomenon of ferrimagnetic resonance has been investigated extensively (ref 1). The application of this phenomenon to the design of microwave narrow-band filters using ferrite (YIG) spheres was first suggested by DeGrasse (ref 2). This original model was later modified to various design configurations electronically tunable over a relatively narrow frequency band (ref 3, 4).

The particular terminal excitation chosen to design a bandpass filter tunable over a very wide frequency range is shown in figure 1. The ferrite sphere is placed in the crossover region O of striplines 3-4 and 1-2, and magnetized to ferrimagnetic reso- nance at a desired operating frequency. Stripline ends 1,2 and 3,4 are then connected to external terminals T_1 and T_2 as shown in figure 1.

The input signal at one terminal is divided into two signals. These two signals, after passing through two different paths, in- teract with each other to give a null in the electric field at the crossover region O. To obtain this electric null over a very wide frequency band, one of the two paths must include a broadband 180-deg phase shifter. This electric null is equivalent to a magnetic field maximum, which is necessary for efficient coupling between the ferrite sphere and the rf signal.

If the input signal has the same frequency as the resonance frequency of the magnetized ferrite sphere, it will be coupled to the other stripline circuit by the ferrite and appear at the output

180-DEGREE PHASE SHIFTER

180-DEGREE PHASE SHIFTER
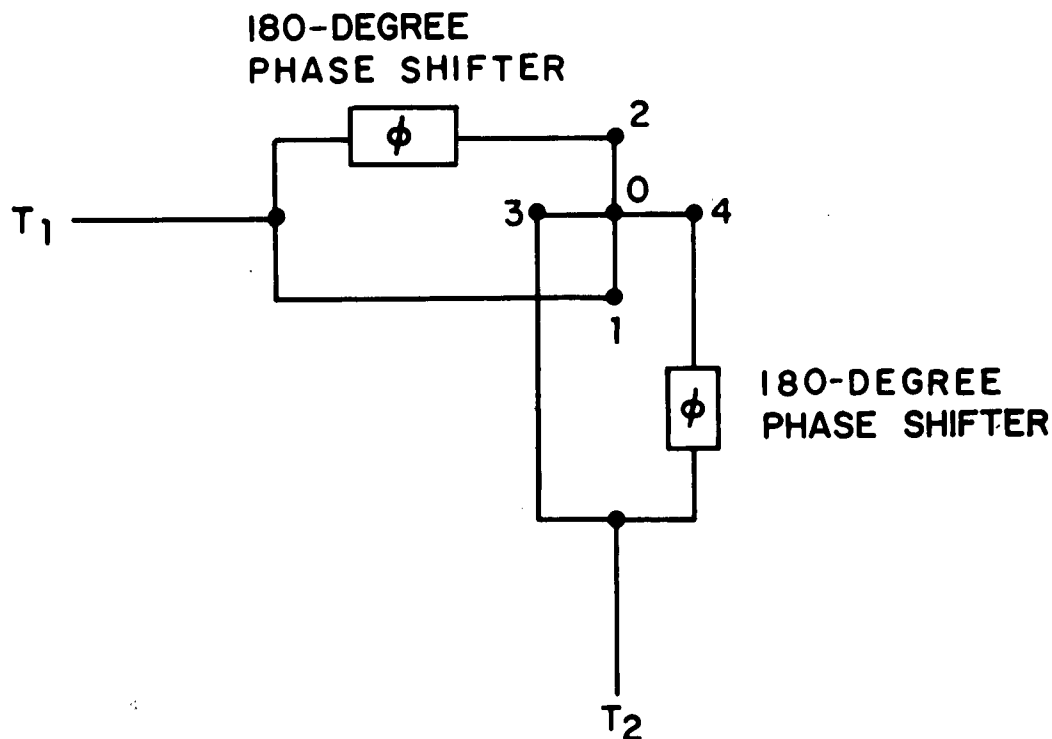
Figure 1. Bandpass filter circuit.

terminal. This report describes the design and evaluation of such a ferrite bandpass filter that is electronically tunable over a very wide frequency range, beginning first with a review of the basic principles of the filter design.

2. BASIC PRINCIPLES

This section describes the theory of operation, electrical properties of ferrite materials, and performance characteristics of an electronically tunable YIG bandpass filter, using the ferrimagnetic resonance phenomena (ref 1). To understand the operation of this YIG filter, it is first necessary to consider the motion of a magnetic moment $\vec{M}$ in the presence of a constant magnetic field $\vec{H}_o$ (fig. 2). When a large static magnetic field is applied to a ferrite material, a torque is exerted on the dipole $\vec{M}$, given by

$$\vec{T} = \vec{M} \times \vec{H}_o,$$
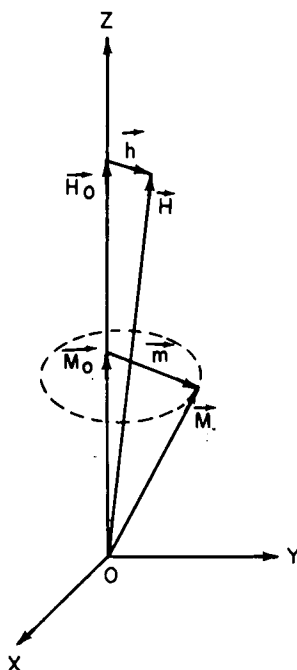
Figure 2. Magnetic dipole in a magnetic field.

resulting in a precession of this electronic dipole moment about $\vec{H}_o$ at a frequency

$$\omega = \gamma \vec{H}_o$$

where γ is a constant (gyromagnetic ratio of the electron). Due to the dissipation of rf energy in the form of heat and re-radiation, the electronic dipoles will in time align themselves with the applied magnetic field $\vec{H}_o$, and the precession will stop.

If, in addition to the large static field $\vec{H}_o$, an rf magnetic field $\vec{h}$ (prependicular to $\vec{H}_o$ and with an amplitude much less than that of $\vec{H}_o$) is applied to the dipole, the dipole will precess around the direction of $\vec{H}_o + \vec{h}$. If $\vec{h}$ is circularly polarized, the vector $\vec{H}_o + \vec{h}$ will describe a cone around the direction OZ, carrying with it the dipole moment with a precessional motion superimposed on it. For the special case when $\vec{h}$ rotates around $\vec{H}_o$ in the same sense and has the same frequency as that of the dipole rotation, ferrimagnetic resonance occurs. This causes the amplitude of the precession angle to increase until the energy supplied by the rf field balances the losses exactly, at which time the motion of the dipole is maintained in equilibrium at the expense of energy absorbed from the rf field. If the rf magnetic field $\vec{h}$ rotates in the opposite sense—even at the same frequency as that of the rotating dipole moment—resonance will not occur. Therefore, at ferrimagnetic resonance, the energy absorbed by the uniform precessional motion will be reradiated,

most of which can be coupled to an external circuit if the dissipation-losses are small.

When the above-described resonance phenomenon is applied to the design of tunable bandpass filters, a number of important factors must be considered. It is desirable to have a constant resonance response, no secondary resonances, very narrow resonance peaks, small heat loss, tight coupling between input and output terminals at all operating frequencies, and minimum coupling during off-resonance. Thus, a good tunable filter depends primarily on the ferrimagnetic material used and the external coupling circuit. Suitable single crystalline materials having low loss and very narrow resonance line width include YIG, GaYIG (gallium-substituted yttrium iron garnet), and lithium ferrite.

Thus far, the YIG material has proved to be the best material for overall performance. Important electromagnetic properties of the YIG materials that affect the filter performance include saturation magnetization ($4\pi M_s$), line width (ΔH), anisotropy field (H_a), and Curie temperature (T_c). These properties are generally frequency and/or temperature sensitive; their significance is implied in the following resonance frequency equation (ref 1).

$$2\pi f_o = \gamma \left[H_o \pm H_a^{eff} + \left(N_t - N_z \right) 4\pi M_s \right]$$

where

f_o = resonant frequency in MHz,

γ = gyromagnetic ratio for the electron $\left(17.6 \times 10^6 \frac{rad}{Oe/sec} \right)$,

H_o = applied static magnetic field for tuning (oersteds),

H_a^{eff} = effective crystalline anisotropy field (Oe), depending on the orientation of H_o,

N_t = transverse demagnetizing factor, and

N_z = demagnetizing factor in the direction of H_o.

For a sphere $N_t = N_z = 1/3$, the equation of resonance is simply

$$2\pi f_o = \gamma H_o \pm H_a^{eff}.$$

The gyromagnetic ratio γ of YIG is both temperature and frequency independent. The anisotropy field H_a^{eff} is temperature dependent

and is due to the preferential alignment of the magnetic dipoles along certain crystalline directions. This directional dependence enables the applied field H_o to be adjusted with respect to a certain preferential crystalline direction so that the effective anisotropy field is zero.

Another limitation on the resonance frequency is its lower limit. For resonance to be effectual, the material must be magnetically saturated. Therefore, for low-frequency operation, the saturation magnetization must be small. The last parameter—the line width— is both frequency and temperature sensitive and is broadened by poor surface polish, impurities, and porosity of the material.

Besides the electromagnetic properties mentioned above, the shape of the YIG will affect the resonance frequency, whereas the size of the sample will determine the spurious responses in addition to the desired resonance response. These spurious responses are due to the higher order spin-wave resonances caused by a nonuniform rf field, propagation through the sample, and the behavior of the sample as a dielectric resonator. The size effect can be minimized by making the sample small compared with the wavelength.

As to the external circuit, the important parameters to be considered are minimum coupling between the input and output ports, maximum coupling during resonance, and provision for mounting the sample so that the metallic-wall effect will not influence the performance. Various circuits have been considered by a number of researchers (ref 1, 2, 3). Their problems have included the requirement of more than one sample, complication of tuning when using more samples, limitation on the tunable bandwidth, and spurious responses.

3.   THEORETICAL ANALYSIS

This section analyses the circuit properties of the two orthogonal strip-transmission lines coupled by a magnetized ferrite sphere, using the scattering matrix method. An equivalent circuit is obtained from the scattering matrix, and one excitation condition of the terminals is shown to be applicable to the design of a very broadband tunable bandpass filter.

The above circuit consists of two striplines, the center conductors of which cross each other at right angles as shown in figure 3. The YIG sphere is located symmetrically in the crossover region between the two center conductors, the size and position of which are chosen such that the rf field will not be disturbed appreciably at off-resonance frequencies. The coordinates and terminal designations are shown in this figure.
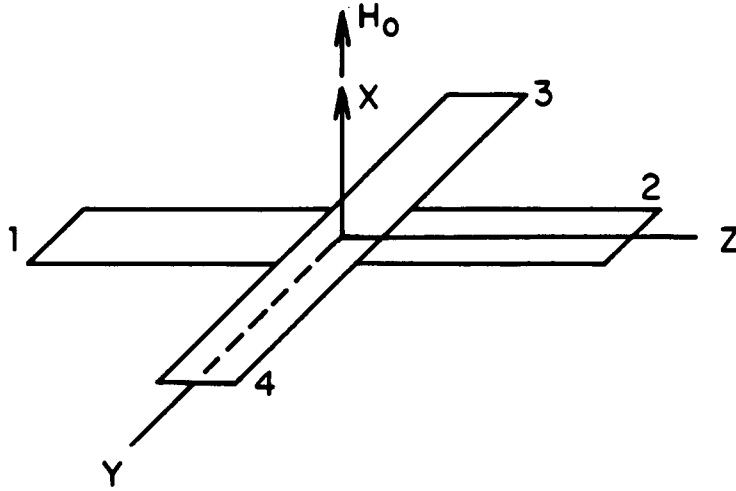
Figure 3. Cross-coupled stripline.

With the applied static magnetic field $\vec{H}_o$ in the X-direction and the YIG biased at magnetic saturation, the susceptibility tensor is given by (ref 1)

$$\chi \;=\; \begin{vmatrix} 0 & 0 & 0 \\ 0 & \chi_{22} & \chi_{23} \\ 0 & -\chi_{23} & \chi_{33} \end{vmatrix}$$

where for negligible loss,

$$\chi_{33} = \chi_{22} = \frac{\omega_o \omega_m}{\omega_o^2 - \omega^2} \;,\quad \chi_{23} = -j\,\frac{\omega \omega_m}{\omega_o^2 - \omega^2}$$

$$\omega_m = 4\pi\gamma M_s \;\;(\text{rad/sec})$$

$$\omega_o = \gamma H_o + H_a^{eff} \;\;(\text{rad/sec})$$

$$\omega = rf \;\; \text{frequency (rad/sec)}.$$

Since the stripline propagates a TEM wave, the magnetic component of the rf field at the YIG sphere is in the Y-direction for strip 1-2 and in the Z-direction for strip 3-4. The positive directions of propagation in the two strips are the same as the directions of

the coordinate axes Y and Z. An rf field is assumed incident at terminal 1, and the other terminals are terminated in matched impedances. When the YIG sphere is in an rf magnetic field, a precessing magnetic dipole moment is induced in it. This dipole moment radiates an rf field which is guided by the external medium. Therefore, the resultant magnetic field at the YIG sphere is not the incident magnetic field only.

Collin has shown (ref 5) that to find the field radiated by an arbitrary magnetic moment $\vec{M}$ in a cylindrical waveguide is to expand the radiated field in terms of a suitable set of normal modes, and to determine the amplitude coefficients in this expansion by an application of the Lorentz reciprocity theorem. His results show that when the field radiated in the forward direction is represented by

$$\vec{E}^{+} = \sum_n a_n \vec{E}_n^{+}$$

$$\vec{h}^{+} = \sum_n a_n \vec{h}_n^{+}$$

and the field radiated in the backward direction is given by

$$\vec{E}^{-} = \sum_n b_n \vec{E}_n^{-}$$

$$\vec{h}^{-} = \sum_n b_n \vec{h}_n^{-}$$

where a_n and b_n are amplitude coefficients and $\vec{E}_n^{-}$, $\vec{h}_n^{-}$, $\vec{E}_n^{+}$, $\vec{h}_n^{+}$ are mode functions in the forward and backward directions, respectively.

Then

$$2b_n = j\omega\mu \, \vec{h}_n^{+} \cdot \vec{M}$$

$$2a_n = j\omega\mu \, \vec{h}_n^{-} \cdot \vec{M},$$

where μ is the permeability of the medium. These results are also valid for coaxial transmission lines.

In the case of strip-transmission lines, only the TEM mode is assumed to propagate and its amplitude is negligibly small at a short distance from the center conductor. Therefore, the stripline can be approximated by a coaxial transmission line and the above analysis can be used. Except for a change of coordinates and their respective vectorial directions, the TEM mode has the same magnetic functional form $\vec{h}$ for all terminals. They also have the same magnitude at the origin of the coordinate system, because the sphere is symmetrically located with respect to the two striplines.

11

The YIG sphere—under the influence of the incident field and reradiating field—can be replaced by two arbitrary orthogonal magnetic dipole moments, M_z and M_y. However, because of the tight coupling which exists between these orthogonal dipole moments in the YIG, it is necessary to impose the condition that the dipole moments induced by M_z and M_y, given by the higher order coupling terms in the equation of motion, cancel each other. For this condition, the effective susceptibility tensor of the YIG sphere which is responsible for creating the moments M_z and M_y must be different when radiation occurs under the excitation of the incident wave.

Let the incident magnetic field at terminal 1 be $A'h\vec{y}$, where $\vec{y}$ is a unit vector in the Y-direction. The resultant magnetic field at the YIG sphere that induces the moments M_z and M_y will be solely determined by the incident wave and the radiation field of M_y, and therefore in the Y-direction. Also, let the effective susceptibility tensor of the YIG sphere be

$$\chi_e = \begin{vmatrix} 0 & 0 & 0 \\ 0 & \chi_{22} & C\chi_{23} \\ 0 & -B\chi_{23} & D\chi_{33} \end{vmatrix}$$

and the resultant magnetic field be $h'\vec{y}$, where B, C, and D are to be determined. The magnetization of the YIG sphere is then given by

$$\vec{m} = \chi_e \cdot h'\vec{y} = \begin{vmatrix} 0 \\ \chi_{22}h' \\ -B\chi_{23}h' \end{vmatrix}$$

If the YIG sphere has a volume V and the applied static and rf magnetic field are uniform inside the ferrite sphere, the total magnetic moment is $M = Vm$. This moment M is considered as a point magnetic dipole moment with components M_z and M_y, situated at the origin O and reradiating rf energy into the external circuit.

From Collin's results, the waves coming from the terminals are given by

terminal 1 $\quad \vec{h}_{11} = b_1\vec{h}_1 = j\frac{1}{2}\omega\mu\,\chi_{22}\,V\,hh'\vec{h}_1$

terminal 2 $\quad \vec{h}_{21} = a_1\vec{h}_2 = -j\frac{1}{2}\omega\mu\,\chi_{22}\,V\,hh'\vec{h}_2$

terminal 3 $\quad \vec{h}_{31} = b_1\vec{h}_3 = j\frac{1}{2}\omega\mu\,\chi_{23}\,V\,hh'\vec{h}_3\,B$

terminal 4 $\quad \vec{h}_{41} = b_1\vec{h}_4 = -j\frac{1}{2}\omega\mu\,\chi_{23}\,V\,hh'\,B\vec{h}_4$

Since it has been assumed that the dipole moments induced by M_z and M_y in the YIG sphere will cancel each other, the resultant Y-component of these induced dipole moments is

$$\chi_{22} \, V\left(j\omega\mu \, \chi_{22} \, V \, h^2 h'\right) + B \, \chi_{23} \, V\left(j\omega\mu \, \chi_{23} \, h^2 \, B \, h'V\right) = 0,$$

where the first term is the Y-component of the dipole induced by the waves in the stripline 1-2, and the second term is the Y-component of the dipole induced by the waves in the stripline 3-4. B is found from this equation to be

$$B = \omega_o/\omega.$$

Since there are no secondary induced dipole moments radiating additional fields, the effective magnetic field at the YIG is

$$h'\vec{y} = \left[A'h - j\tfrac{1}{2}\left(\omega\mu \, V\chi_{22} \, h^2 h'\right) - j\tfrac{1}{2}\left(\omega\mu \, V\chi_{22} \, h^2 h'\right)\right]\vec{y},$$

where the first term is the magnitude of the incident wave, the second term is the magnitude of the reflected wave, the third term is the magnitude of the transmitted wave, and their respective vectorial directions have been included in the signs before each term.

Solving for h',

$$h' = A'h/(1 + j\omega\mu \, \chi_{22} \, Vh^2),$$

where $A'h$ is the amplitude of the incident magnetic field.

Finally, taking the reference plane at the YIG sphere, the waves coupled to the four terminals for an incident rf field at terminal 1 are obtained from Collin's results:

Incident: $\vec{y} \, A'h e^{-\beta z}$

Reflected: $h_{11} = \vec{y}\left[\dfrac{j\tfrac{1}{2}\omega\mu \, \chi_{22} V \, h^2}{1+j\omega\mu\chi_{22}V \, h^2}\right]\left(-A'h\right) e^{\beta z}, \quad z \leq 0$

Transmitted: $h_{21} = \vec{y}\left[1 - \dfrac{j\tfrac{1}{2}\omega\mu \, \chi_{22} \, V \, h^2}{1+j\omega\mu \, \chi_{22} \, V \, h^2}\right]\left(A'h\right) e^{-\beta z}, \quad z \geq 0$

Terminal 3: $h_{31} = \vec{z}\left[\left(\dfrac{\omega_o}{\omega}\right)\dfrac{j\tfrac{1}{2}\omega\mu \, \chi_{23} \, V \, H^2}{1+j\omega\mu \, \chi_{22}V \, H^2}\right]\left(A'h\right) e^{\beta y}, \quad y \leq 0$

Terminal 4: $h_{41} = \vec{z}\left[-\dfrac{j\tfrac{1}{2}\omega\mu \, \chi_{23} \, V \, H^2}{1+j\omega\mu \, \chi_{22}V \, H^2}\left(\dfrac{\omega_o}{\omega}\right)\right]\left(-A'h\right)e^{-\beta y}, \quad y \geq 0$

where $\vec{x}$, $\vec{y}$, $\vec{z}$ denote the unit vectors in the X-, Y-, Z-directions, respectively. When a similar analysis is applied to the other terminals and letting

$$s_1 = \frac{j\frac{1}{2}\omega\mu\chi_{22}Vh^2}{1 + j\omega\mu\chi_{22}Vh^2} \; ,$$

$$s_2 = \left(\frac{\omega_o}{\omega}\right)\frac{j\frac{1}{2}\omega\mu\chi_{23}Vh^2}{1 + j\omega\mu\chi_{22}Vh^2} \; ,$$

a_1, a_2, a_3, a_4 = the magnitudes of the incident waves at the respective terminals, and

b_1, b_2, b_3, b_4 = the magnitudes of the waves travelling away from the YIG sphere to the respective terminals;

the input and output are related by the scattering matrix

$$\begin{vmatrix} b_1 \\ b_2 \\ b_3 \\ b_4 \end{vmatrix} = \begin{vmatrix} s_1 & 1-s_1 & -s_2 & s_2 \\ 1-s_1 & s_1 & s_2 & -s_2 \\ s_2 & -s_2 & s_1 & 1-s_1 \\ -s_2 & s_2 & 1-s_1 & s_1 \end{vmatrix} \begin{vmatrix} a_1 \\ a_2 \\ a_3 \\ a_4 \end{vmatrix}$$

Substituting the expressions for χ_{22} and χ_{23} to obtain s_1 and s_2,

$$s_1 = \frac{j\dfrac{\omega\mu\omega_o\omega_m Vh^2}{2(\omega_o^2 - \omega^2)}}{1 + j\omega\mu\dfrac{\omega_o\omega_m Vh^2}{\omega_o^2 - \omega^2}}$$

$$s_1 \Big|_{j\omega=p} = \frac{\dfrac{A}{2}p}{p^2 + Ap + \omega_o^2}$$

where $A = \mu\omega_o\omega_m Vh^2$

and $s_2 = \dfrac{j\frac{1}{2}\omega\mu(-j\chi_{22})Vh^2}{1 + j\omega\mu\chi_{22}Vh^2} = -js_1$

14

The magnitudes of the elements for the above scattering matrix are less than unity. To realize the scattering matrix with passive circuit elements, $1 - \tilde{S}S \geq 0$, where $\tilde{S}$ denotes the conjugate transpose of S.

Thus,

$$\tilde{S}S = \begin{vmatrix} s_1^* & 1-s_1^* & js_1^* & -js_1^* \\ 1-s_1^* & s_1^* & -js_1^* & js_1^* \\ -js_1^* & js_1^* & s_1^* & 1-s_1^* \\ js_1^* & -js_1^* & 1-s_1^* & s_1^* \end{vmatrix} \begin{vmatrix} s_1 & 1-s_1 & js_1 & -js_1 \\ 1-s_1 & s_1 & -js_1 & js_1 \\ -js_1 & js_1 & s_1 & 1-s_1 \\ js_1 & -js_1 & 1-s_1 & s_1 \end{vmatrix}$$

where s^* denotes the conjugate of s. Multiplying the two matrices together and simplifying, it is found that

$$\tilde{S}S = \begin{vmatrix} 1 & 0 & 0 & 0 \\ 0 & 1 & 0 & 0 \\ 0 & 0 & 1 & 0 \\ 0 & 0 & 0 & 1 \end{vmatrix}$$

4.   SYNTHESIS OF EQUIVALENT FILTER CIRCUIT

When attempting to realize the scattering matrix S derived above, it is found that both the admittance and impedance matrices do not exist and, therefore, S cannot be realized by the admittance or impedance method. To synthesize by the scattering matrix method, the following procedure is used (ref 6,7). The augmented admittance matrix Y_A of the scattering matrix S is given by $Y_A = \frac{1}{2}(E - S)$; that is,

$$Y_A = \frac{1}{2} \begin{vmatrix} 1-s_1 & -(1-s_1) & -js_1 & js_1 \\ -(1-s_1) & 1-s_1 & js_1 & -js_1 \\ js_1 & -js_1 & 1-s_1 & -(1-s_1) \\ -js_1 & js_1 & -(1-s_1) & 1-s_1 \end{vmatrix}$$

where E is the identity matrix. This augmented admittance matrix can be diagonalized by a unitary transformation given by

$$u = \frac{1}{2} \begin{vmatrix} 1 & 1 & 1 & 1 \\ -1 & 1 & 1 & -1 \\ j & 1 & -1 & -j \\ -j & 1 & -1 & j \end{vmatrix}$$

15

Thus,

$$\widetilde{U} \ Y_A \ U = \begin{vmatrix} 1 & 0 & 0 & 0 \\ 0 & 0 & 0 & 0 \\ 0 & 0 & 0 & 0 \\ 0 & 0 & 0 & (1-2s_1) \end{vmatrix}$$

Since $S = E - 2Y_A$ and $\hat{S} = \widetilde{U}SU = E - 2\widetilde{U}Y_AU,$

$$\hat{S} = \begin{vmatrix} -1 & 0 & 0 & 0 \\ 0 & 1 & 0 & 0 \\ 0 & 0 & 1 & 0 \\ 0 & 0 & 0 & (4s_1-1) \end{vmatrix}$$

This diagonal matrix $\hat{S}$ represents a four-port network where the input reflection coefficient of each port is given by the value of the respective diagonal element. For the fourth port, the reflection coefficient Γ is $(4s_1-1)$. Therefore, the input impedance of this port is

$$Z = \frac{1 + \Gamma}{1 - \Gamma} = \frac{2s_1}{1-2s_1}$$

Since $s_1 = \dfrac{\frac{A}{2} p}{P^2 + Ap + \omega_o^2}$, where $p = j\omega,$

then,

$$Z = Ap/(p^2 + \omega_o^2),$$

which represents a parallel-resonant circuit as shown in figure 4.
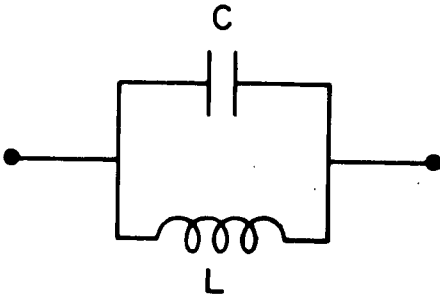
$$C = \frac{1}{A} = \frac{1}{\mu \, \omega_0 \, \omega_m \, V h^2}$$

$$L = \frac{A}{\omega_0^2} = \frac{\mu \, \omega_m \, V h^2}{\omega_0}$$

Figure 4. Equivalent parallel-resonant circuit.

16

The second and third ports of $\hat{S}$ are open circuited, whereas the first port is a short circuit.

To convert the circuit for $\hat{S}$ to the network represented by S, it is seen that $\widetilde{U}SU = \hat{S}$. If $\hat{v}$, $\hat{i}$ represent the voltage and current, respectively, for network $\hat{S}$, then

$$(\hat{V}-\hat{i}) = (\widetilde{U}SU)(\hat{V}+\hat{i}) = \hat{S}(\hat{V} + \hat{i})$$

and

$$U(\hat{V}-\hat{i}) = S\,[U(\hat{V} + \hat{i})].$$

Also, $(V-i) = S(V + i)$

where v, i are the normalized voltage and current for network S. Therefore,

$$V = \tfrac{1}{2}[(v + i) + (v-i)] = \tfrac{1}{2}U[(\hat{v}+\hat{i})+ (\hat{v}-\hat{i})] = U\hat{V}$$

$$\hat{i} = \tfrac{1}{2}[(\hat{v} + \hat{i}) - (\hat{v}-\hat{i})] = \tfrac{1}{2}\widetilde{U}[(v+i)-(v-i)] = \widetilde{U}i$$

Thus, the network for S is obtained by connecting a multiport ideal transformer U to $\hat{S}$.

It is observed in U that an ideal transformer with complex turns ratio (shown in top of figure 5) is required. This transformer can be decomposed into the configuration shown in bottom of figure 5, where the complex transformer at the center represents a nonreciprocal lossless phase shifter. The proof of this is shown by defining a generalized gyrator

$$V_2 = \alpha I_i$$

$$V_1 = -\alpha^* I_2$$

where α is complex and equals $e^{j\theta}$. If the magnitude of α is not unity, real transformers of appropriate turns ratio can be extracted so that α is reduced to the form of $e^{j\theta}$.

The impedance matrix Z for the generalized gyrator is

$$Z = \begin{vmatrix} 0 & -\alpha^* \\ \alpha & 0 \end{vmatrix},$$

while its scattering matrix is

$$S = (Z - E)(Z + E)^{-1}$$

$$= \tfrac{1}{2} \begin{vmatrix} 0 & -2\alpha^* \\ 2\alpha & 0 \end{vmatrix} = \begin{vmatrix} 0 & -e^{-j\theta} \\ e^{j\theta} & 0 \end{vmatrix}$$
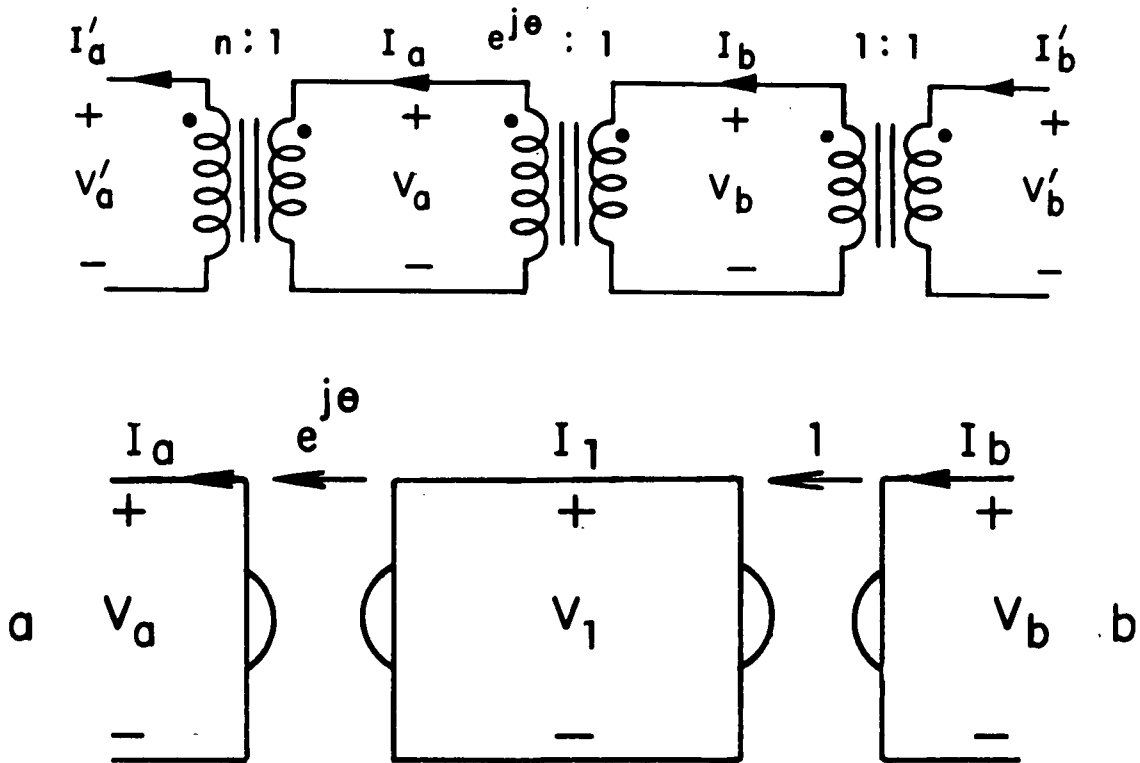

Figure 5. Complex ideal transformer circuit.

This shows that the rf wave in going from port 1 to 2 has a phase shift of $-\theta + 180$ deg while the wave from port 2 to 1 has a phase shift of θ deg. This generalized gyrator is lossless and passive because

$$\widetilde{S}S = \begin{vmatrix} 0 & e^{-j\theta} \\ e^{j\theta} & 0 \end{vmatrix} \begin{vmatrix} 0 & -e^{-j\theta} \\ e^{j\theta} & 0 \end{vmatrix} = \begin{vmatrix} 1 & 0 \\ 0 & 1 \end{vmatrix}$$

The complex ideal transformer can now be synthesized by extracting generalized gyrators so that the final network has the same terminal characteristic as that of the ideal complex transformer, resulting in the gyrator network shown in figure 5. The terminal characteristics of such a gyrator network are given by

$$I_a = e^{j\theta} V_1 = e^{j\theta} I_b = \frac{I_b}{(e^{j\theta})^*}$$

$$V_a = e^{j\theta} I_1 = e^{j\theta} V_b,$$

which are the same as that for the ideal complex transformer. Thus, when an incident wave travels from port b to port a, its phase changes by θ deg; whereas, for an incident wave travelling in the opposite direction, the phase change is $(-\theta + 180 + 180)$ or $-\theta$ deg. Therefore, an ideal complex transformer with a complex turns ratio of $e^{j\theta}:1$ is a nonreciprocal phase shifter, having a differential phase shift of 2θ deg.

With an ideal complex transformer now defined, the multiport ideal transformer U or the YIG filter scattering matrix S can be found. The voltage relation connecting the network of $\hat{S}$ and the network of S is given by $V = U\hat{V}$. Expanding this relationship results in

$$V_1 = \tfrac{1}{2}(\hat{V}_1 + \hat{V}_2 + \hat{V}_3 + \hat{V}_4)$$

$$V_2 = \tfrac{1}{2}(-\hat{V}_1 + \hat{V}_2 + \hat{V}_3 - \hat{V}_4)$$

$$V_3 = \tfrac{1}{2}(j\hat{V}_1 + \hat{V}_2 - \hat{V}_3 - j\hat{V}_4)$$

$$V_4 = \tfrac{1}{2}(-j\hat{V}_1 + \hat{V}_2 - \hat{V}_3 + j\hat{V}_4)$$

which is represented by the equivalent circuit of the cross-coupled tunable YIG filter shown in figures 9 and 10 of reference 8.

5.   DESIGN OF 180-DEGREE PHASE SHIFTERS

The analysis given in section 4 shows that if equal and out-of-phase signals are fed into the opposite terminals of two orthogonal striplines coupled by a YIG sphere, equal and out-of-phase signals will appear at the other two terminals when the YIG sphere is magnetized to ferrimagnetic resonance. To provide 180-deg phase difference between the signals over a wide bandwidth, broadband phase shifters are required.

A circuit consisting of two paths differing by a multiple of half-wave-lengths is inherently narrowband. However, the design of a broadband 90-deg phase shifter, given by Schiffman (ref 9) and later

extended by Cristal and Shelton (ref 10, 11), is applicable to the
solution of the above problem. The basic configuration of this broad-
band phase shifter consists of a section of coupled lines as shown at
the top of figure 6.

The image impedance Z_1 and the phase shift ϕ of the Shiffman
model—called the phase section—are given by

$$Z_1 = \sqrt{Z_{oo}Z_{oe}}$$

$$\cos \phi = \frac{\dfrac{Z_{oe}}{Z_{oo}} - \tan^2 \theta}{\dfrac{Z_{oe}}{Z_{oo}} + \tan^2 \theta} ,$$

where Z_{oe} is the characteristic impedance of one line to ground when
equal in-phase currents flow in both lines, Z_{oo} is the characteristic
impedance of one line to ground when equal out-of-phase currents flow
in both lines, and $\theta = \beta L$ is the electrical length of a uniform line
of length L and phase constant β.

The phase shift ϕ, with $\rho = Z_{oe}/Z_{oo}$ as a function of θ is given
at the bottom of figure 6. The phase of a uniform line of length
3L and a coupled line of impedance ratio $\rho = 3$ are compared in
figure 7. The difference in this phase ϕ is given in figure 8.
These results show that by choosing the length of the uniform line
and the impedance ratio ρ of the coupled section, the difference
in phase between the two lines can be nearly constant over a broad
frequency band.

The deviation of the phase difference from the constant value
in the operating band can be further minimized by connecting error-
correcting networks or additional coupled lines to the terminals of
the phase section (figure 9). The extent to which the variation of
phase difference can be minimized and operating band can be broadened
is limited by the mechanical tolerance of this phase section, the
transmission-line losses, and the junction effects.

From mechanical and bandwidth considerations, a 180-deg phase
shifter was fabricated by cascading four 45-deg phase shifters with
a 5:1 bandwidth and 1.0046-deg ripple, the design parameters of which
are given in references 10 and 11. The arrangement of the 180-deg
phase shifter designed for 1.5- to 7.5-GHz frequency range, using
teflon fiberglass as the dielectric medium, is shown in figure 10.
The center conductor, represented by the solid lines, is etched on one
side of a 1/64-in. thick teflon-fiberglass board and is connected
electrically at the ends to the center conductor (represented by the
dotted lines) on the opposite side of the board. This board is then
placed between two 1/16-in. boards (center of fig. 10) where the two

20

outer solid lines represent the ground plane, and the two other lines represent the center conductors of the phase section. The phase difference between the paths along the two arms ACO and ABO is designed for 180 ± 4 deg over the desired operating bandwidth.
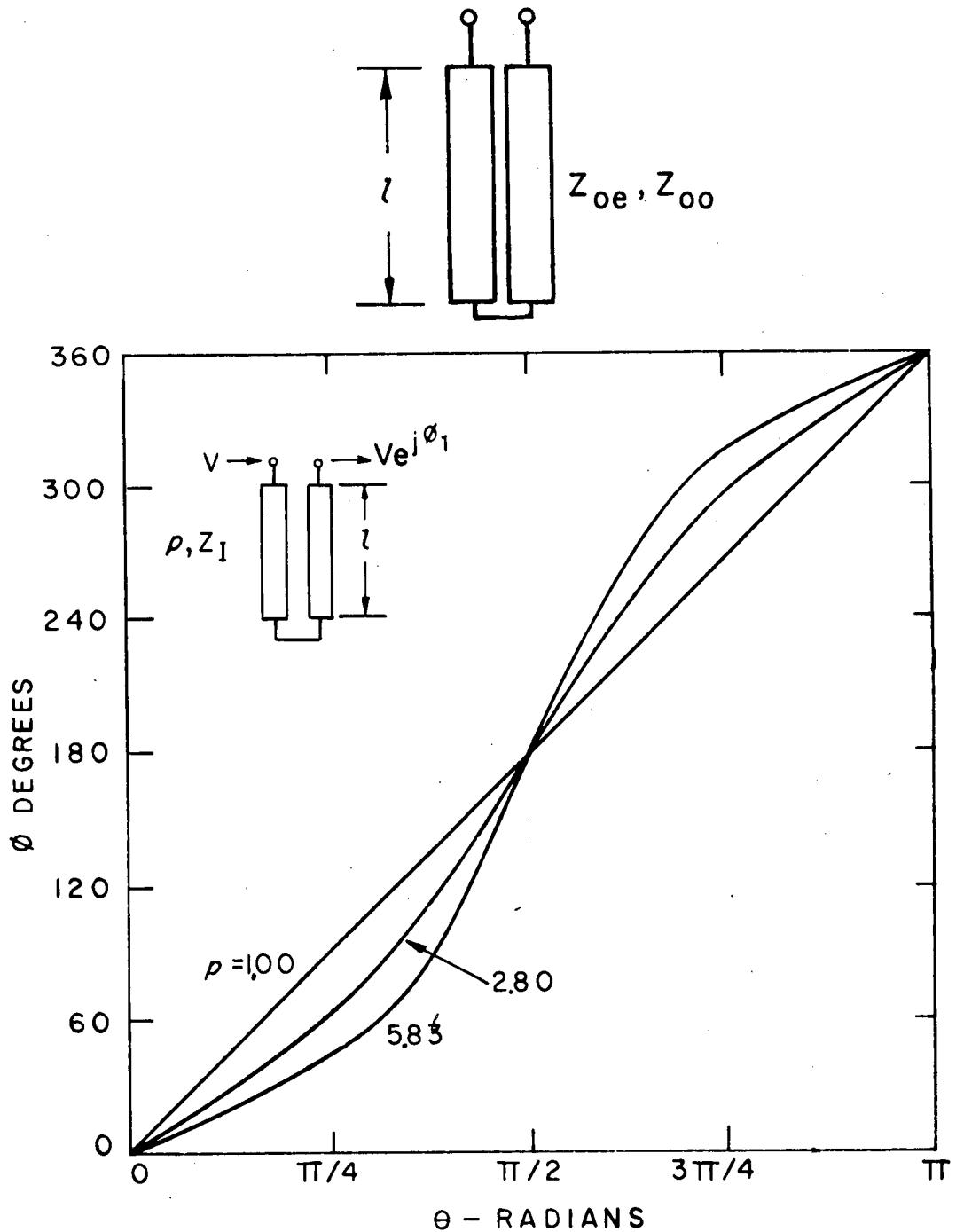

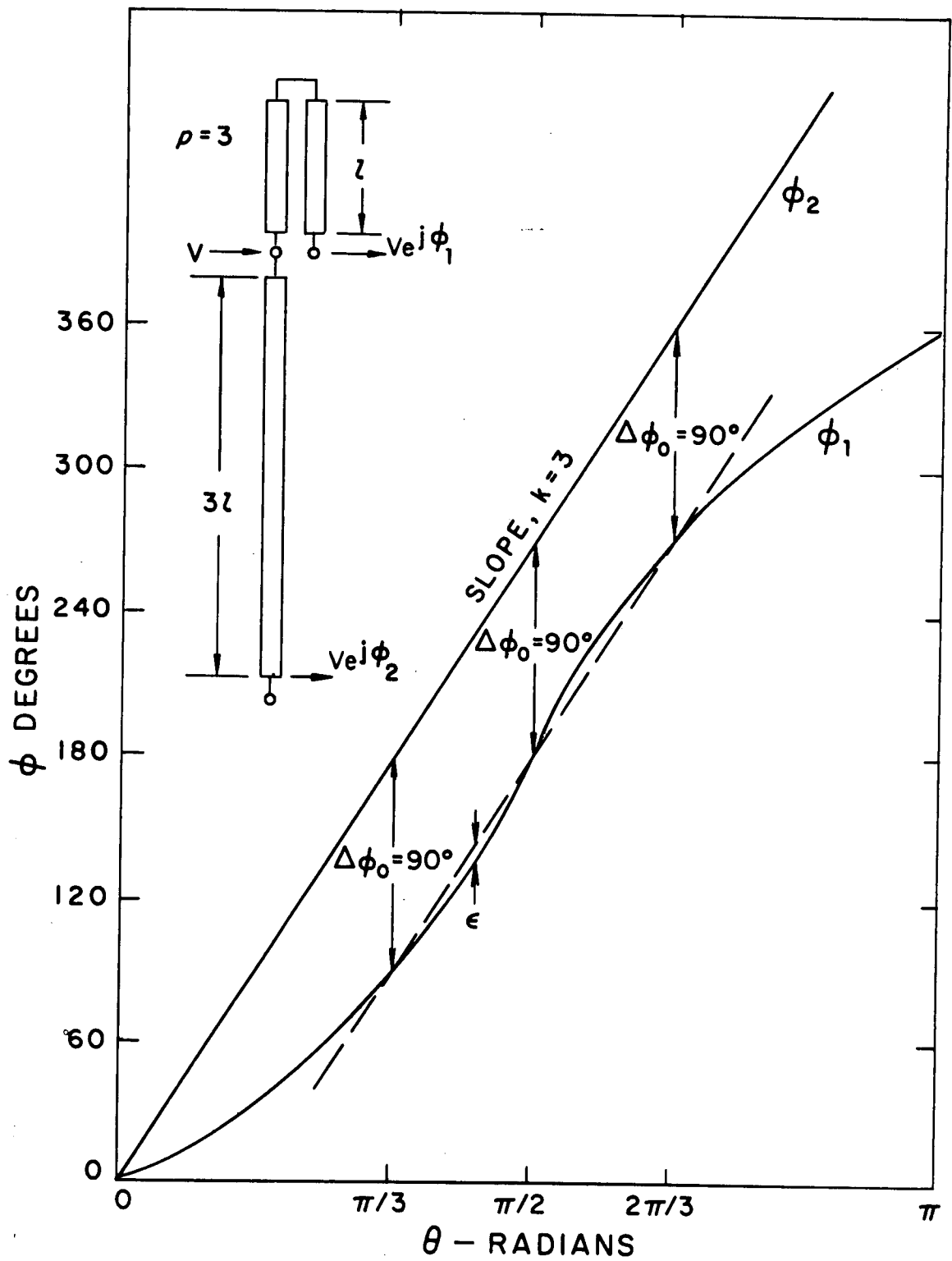Figure 6. Phase shift versus electrical line length.

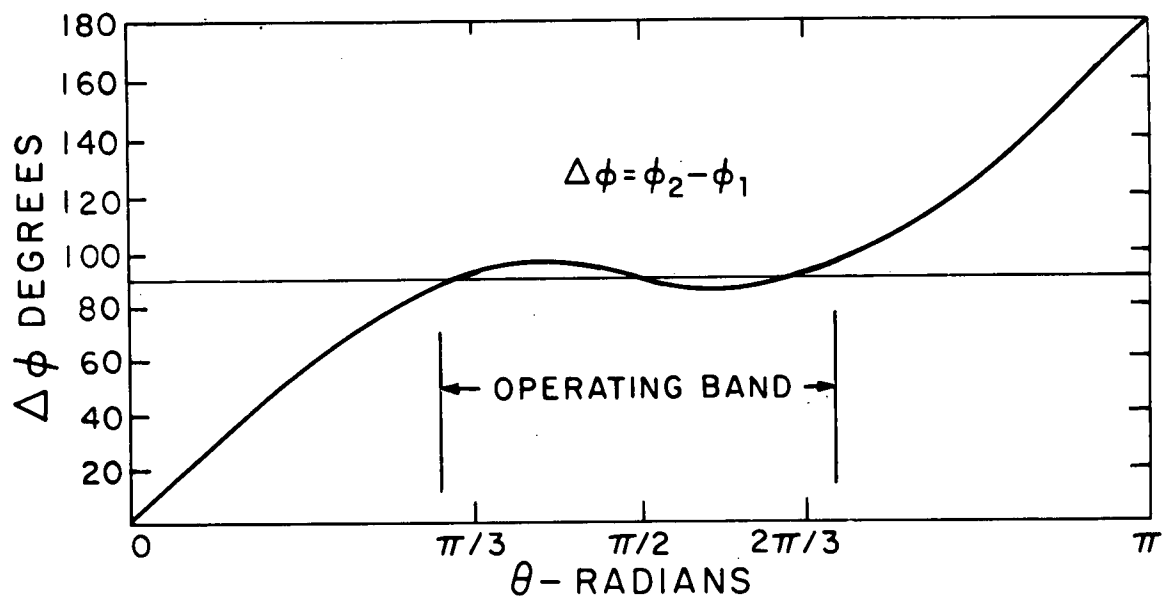Figure 7.   Characteristics of a 90-deg phase shifter.
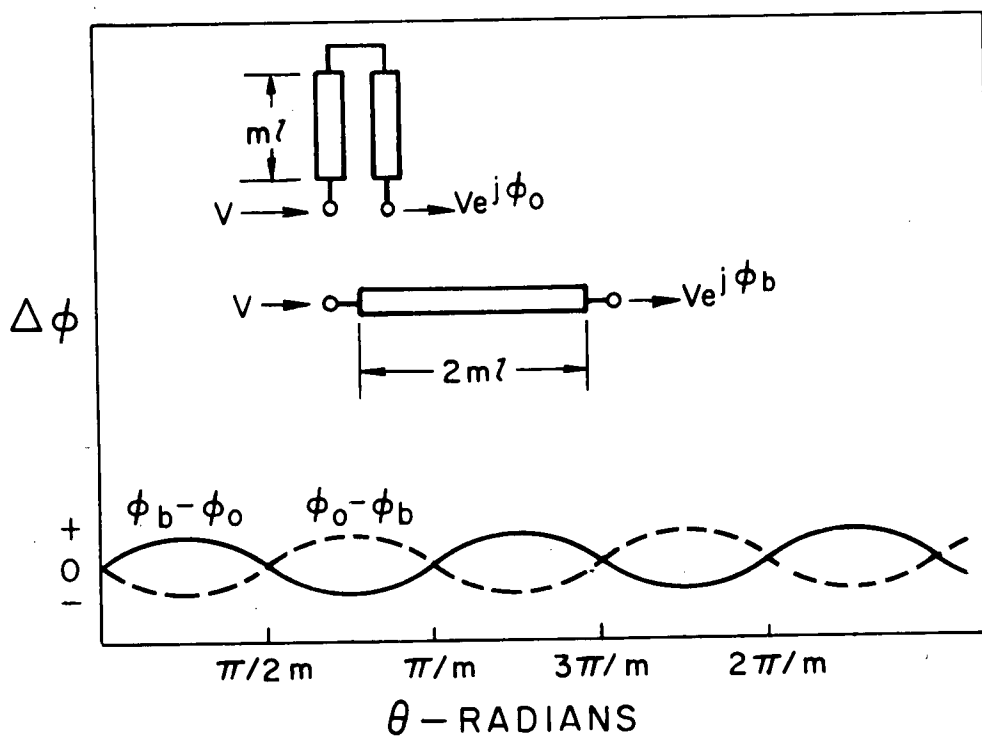
Figure 8.   Phase shift versus electrical line length.

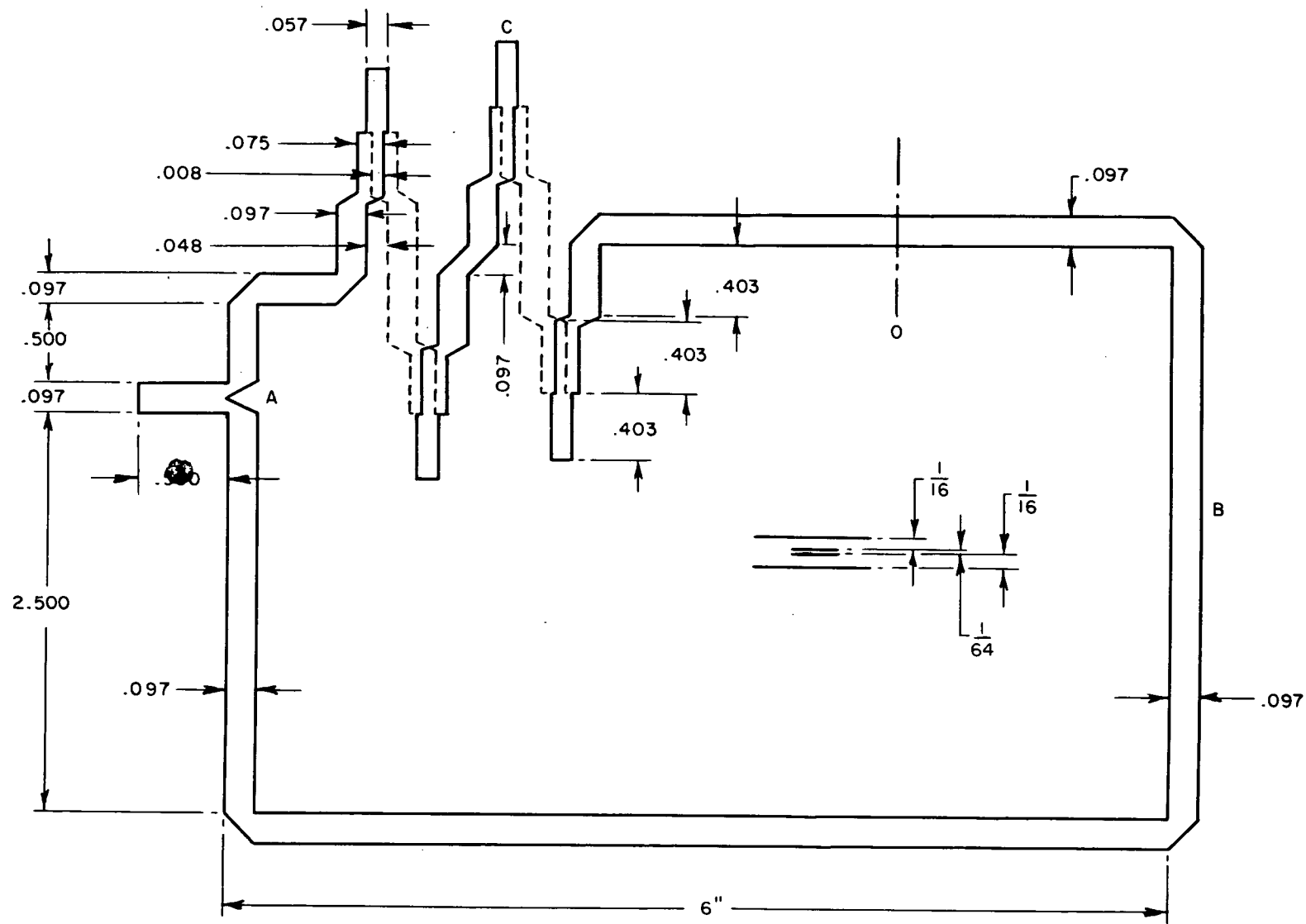
Figure 9.   Design characteristic of error-correcting network.

Figure 10. A 180-deg phase-shift circuit.

6. EXPERIMENTAL EVALUATION

The performance of the YIG bandpass filter depends primarily on the accuracy of the 180-deg phase shifter circuit to obtain an electrical null at the overlapping point 0 as mentioned in section 1. To evaluate the phase shifter circuit as designed in section 4, the experimental setup shown in figure 11 is used. As seen in this figure, the input power is divided into two equal signals, one passing through the 180-deg phase shifter and interacting with the signal in the other arm to give an electric null at point 0. To determine the position of this null, a tapered coplanar stripline probe is used to sample the rf power, the tip of which is a distance from the stripline center conductor at least equal to its width. The axes of the probe and center conductor are perpendicular to each other, the probe being able to slide a small distance parallel to the axis of this stripline center conductor. The stub tuner is used for impedance matching the probe to the detector for maximum sensitivity of the measuring system, and the isolator is used to minimize the reactive loading of the phase shifter on the rf generator.

Denoting the probe position as + and - with respect to the point 0 (shown in fig. 11), the experimental results of the two 180-deg phase shifters are given in figure 12. The deviation, in degrees from the desired 180-deg phase difference at the point 0, is given in millimeters from the reference null point 0. The 45- and 90-deg deviations are also shown in this figure as dotted lines symmetrical about the new reference null position for comparison. The results of these data show that the reference null should be -5 mm from the original position. Possible causes of the large deviations are probably due to the reactive effect of the bends and junctions, and inaccuracy in the etching process of the phase-shift networks.

To assemble a YIG bandpass filter, the two 180-deg phase shifters are cross coupled so that the new reference points 0 of each circuit overlap. A suitable hole is then made between these two points to accommodate the YIG sphere, oriented with its easy axis perpendicular to the plane of the phase circuit by a strong magnetic field while it is loosely held in this position.

Results of the insertion-loss measurements (using substitution method) made on the above bandpass filter at near resonance frequencies are given in figure 13. Although the insertion loss of this first test model was relatively high and its bandwidth varied over the design frequency range, these first results do show that the above phase shifter-YIG bandpass filter is capable of operating effectively over a very wide frequency range. Figure 14 shows the model used to obtain these results.
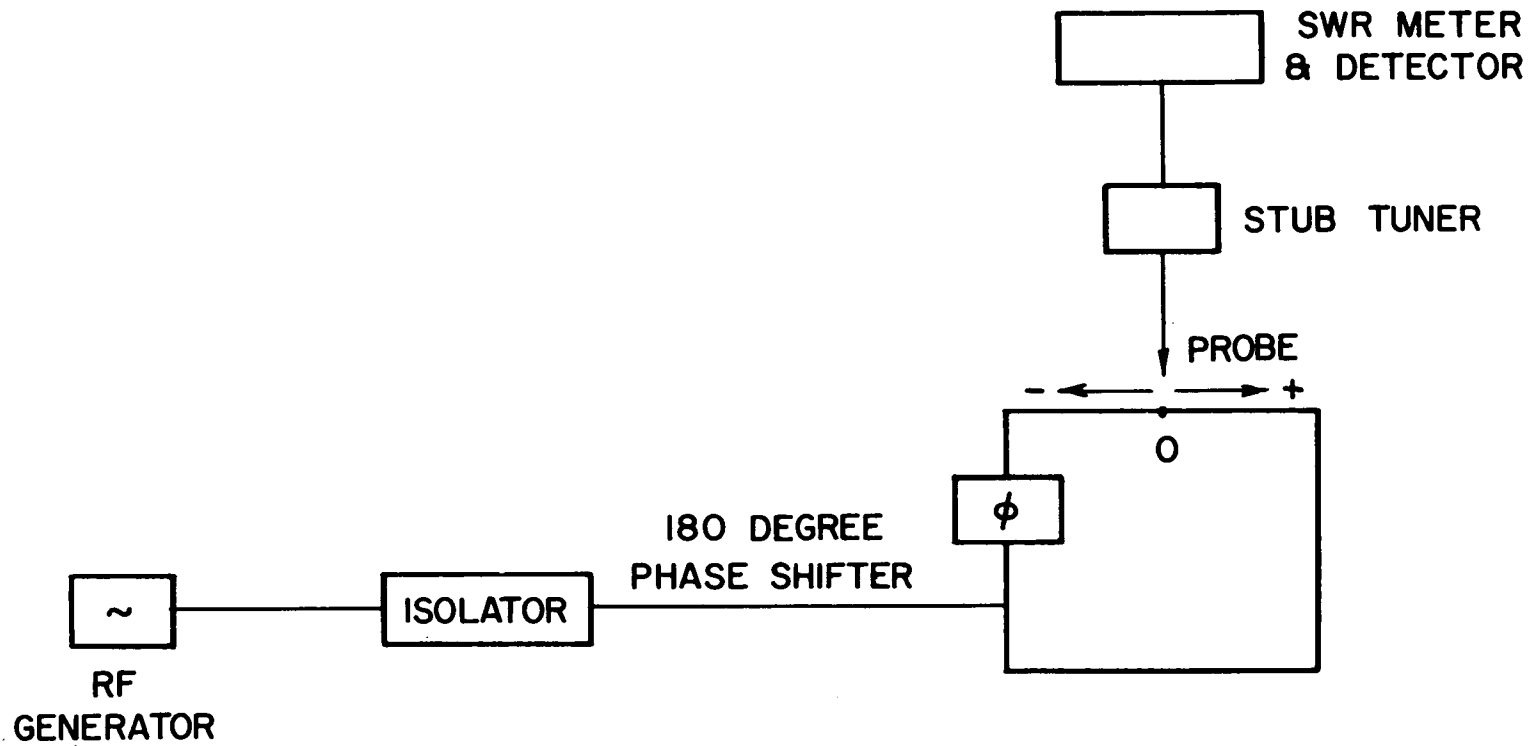
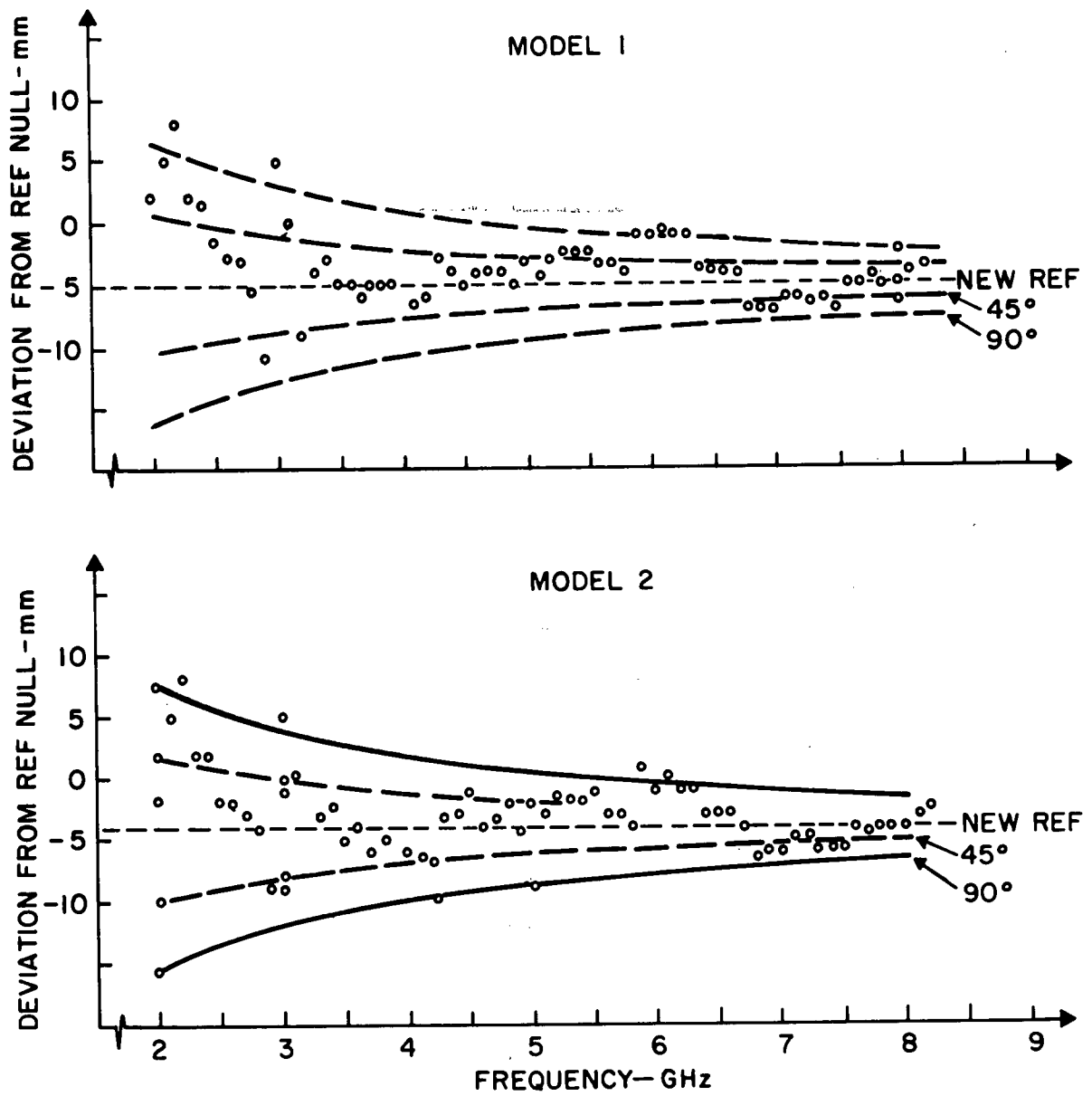Figure 11. Experimental setup for evaluation of 180-deg phase shifter.

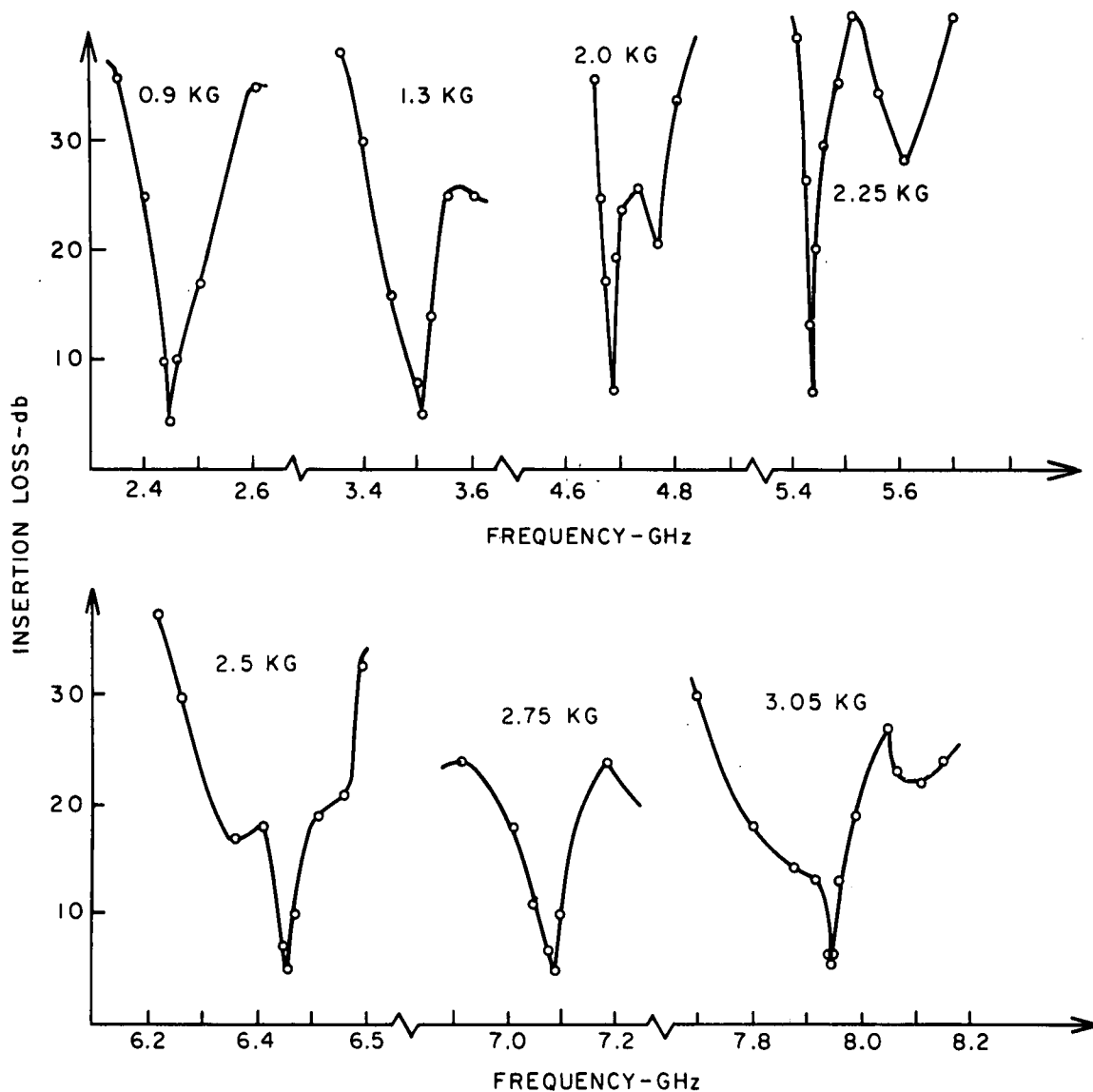Figure 12. Performance of 180-deg phase shifter.

Figure 13. Performance of YIG filter.

Assuming that a 45-deg deviation from 180-deg phase difference exists at the new reference null position, an insertion loss of only 1.5 dB is calculated from the scattering matrix of the filter at resonance. Also assuming the copper loss, reflection loss of the phase shifters, and the dissipation loss of the YIG sphere together equal 1.5 dB, the remaining losses are probably due to insufficient coupling and the generation of higher order modes caused by non-uniform fields in the YIG sphere region. An Airtron 112-225 YIG
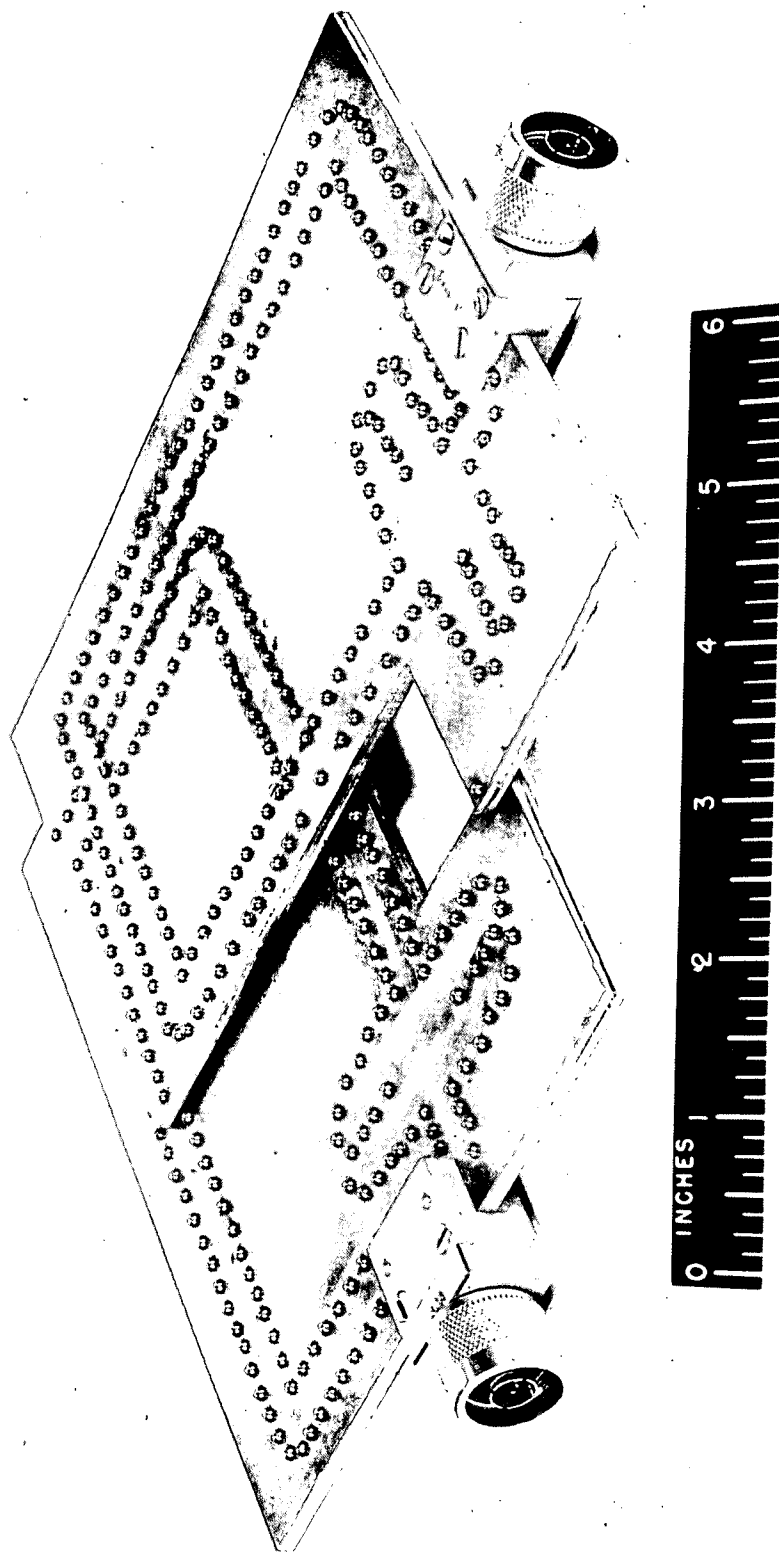
Figure 14. Tunable YIG bandpass filter.

923-1967

29

sphere (0.053 in. diam and a resonance line width of 0.5 Oe) was used for the above measurements.

Design modifications of the above tunable bandpass filter have been completed for minimizing the phase errors caused by the reactive effects of the junctions and bends, and the inaccuracies of the etching process used to fabricate the phase-shift network. This later design model, using 1/8-in. ground plane spacing, was fabricated and evaluated over the operating frequency range of 2 to 8 GHz. The results obtained include an insertion loss of 4 ± 1 dB at all resonant frequencies and an isolation of greater than 30 dB at the off-resonant frequency over the entire operating bandwidth. Further improvements in the performance of this tunable bandpass filter are expected in a final design model (being fabricated) by more carefully aligning the stripline circuitry associated with the 180-deg phase shifter.

7. CONCLUSIONS

The theoretical analysis and experimental results evolving from this investigation indicate the feasibility of designing a YIG bandpass filter, magnetically tunable over more than a 4:1 frequency range. The limit of the tunable bandwidth is determined by the practical difficulties in the fabrication of the 180-deg phase shifters and the magnetic properties of the YIG sphere, including its size. The upper frequency limit is set by the reactive discontinuities and mechanical tolerances of the phase-shift circuits, whereas the lower frequency limit is determined by the saturation magnetization of the YIG sphere.

8. REFERENCES

(1) B. Lax and K. J. Button, "Microwave Ferrite and Ferrimagnetics," Ch 17, McGraw Hill Book Co., Inc., 1964.

(2) R. W. DeGrasse, "Low-Loss Gyromagnetic Coupling Through Single Crystal Garnets," J. Appl. Phys., Vol 30, pp 155s-156s, Apr 59.

(3) L. Matthaei, L. Young and E.M.T. Jones, "Microwave Filters, Impedance-Matching Networks, and Coupling Structures," Ch 17, McGraw Hill Book Co., Inc., 1964.

(4) R. L. Comstock, "Synthesis of Filter-Limiters Using Ferrimagnetic Resonators," IEEE Trans of Microwave Theory and Techniques, MTT-12, No. 6, pp 599-607, Nov 1964.

(5) R. E. Collin, "Field Theory of Guided Waves," pp 198-204, McGraw Hill Book Co., Inc., 1960.

(6) D. Youla, "Direct Single Frequency Synthesis From a Pre-scribed Scattering Matrix," IRE Trans on Circuit Theory CT-6, No. 4, pp 340-344, Dec 1959.

(7) H. J. Carlin and A. B. Giordano, "Network Theory—An Introduction To Reciprocal and Nonreciprocal Circuits," Prentice-Hall Inc., 1964.

(8) T. H. Mak, "Design of Very Broadband Magnetically Tunable YIG Bandpass Filter," MS (Electrophysics) Thesis, Polytechnic Inst of Brooklyn, June 1967.

(9) B. M. Schiffman, "A New Class of Broadband Microwave 90-De-gree Phase Shifters," IRE Trans on Microwave Theory and Techniques, Vol MTT-6, No. 2, pp 232-237, Apr 1958.

(10) E. G. Cristal, "Analysis and Exact Synthesis of Cascaded Commensurate Transmission-Line C-Section All-Pass Networks," IEEE Trans of Microwave Theory and Techniques, Vol MTT-14, No. 6, pp 285-291, June 1966.

(11) J. P. Shelton and J. A. Mosko, "Synthesis and Design of Wideband Equal-Ripple TEM Direction Couplers and Fixed Phase Shifters," IEEE Trans on Microwave Theory and Techniques, Vol MTT-14, No. 10, pp 462-473, Oct 1966.

DISTRIBUTION

Commanding General
U.S. Army Materiel Command
Washington, D. C.   20315
  Attn: AMCRD-DE, M. T. Hedman
  Attn: AMCPP-CM-MI
  Attn: Dr. Jay Tol Thomas, Director, Res & Lab

Office of the Chief of Research & Development
Department of the Army
Washington, D. C.   20310
  Attn: Capt J. M. Kierman, Rm 3E437

Redstone Scientific Information Center
U.S. Army Missile Command
Redstone Arsenal, Alabama   35809
  Attn: Chief, Documents Section

Commanding Officer
Picatinny Arsenal
Dover, New Jersey 07801
  Attn: Library, SMUPA-VA-6

Commanding Officer
U.S. Army Electronics Research & Development Laboratory
Fort Monmouth, New Jersey 07703
  Attn: Electronic Components Research Dept
  Attn: Tech Library

Commanding Officer
U.S. Army Research Office
Box CM, Duke Station
Durham, North Carolina   27700

Commanding Officer
U.S. Army Electronics Research Unit
P.O. Box 205, Mountain View, Santa Clara, California   94040
  Attn: SELRU 3

Commanding Officer
Naval Weapons Center, Corona Laboratories
Corona, California   91720
  Attn: Documents Librarian/Glenn Sharp

Commander
U.S. Naval Ordnance Laboratory
White Oak, Silver Spring, Maryland   20910
  Attn: Tech Library

33

DISTRIBUTION (Continued)

Department of the Navy
Bureau of Naval Weapons
Washington, D. C. 20360
  Attn: DLI-3, Tech Library

Commander
Naval Research Laboratory
Washington, D. C. 20390
  Attn: Microwave Antennas & Components Br
  Attn: Tech Library

Headquarters
Defense Documentation Center
5010 Duke Street
Alexandria, Virginia 22314
  Attn: DDCIR (20 copies)

National Bureau of Standards
Washington, D. C. 20234
  Attn: Library

Boulder Laboratories
National Bureau of Standards
Boulder, Colorado 80302
  Attn: Library

Aero Geo Astro Corporation
4810 Calvert Road
College Park, Maryland 20740

Radiation System, Inc.,
1755 Old Meadow Road
McLean, Virgina 22101

International Telephone & Telegraph Labs
Fort Wayne, Indiana 46801
  Attn: Paul R. Jordan/R. Bartel

USASRDL
Fort Monmouth
Eatontown, New Jersey 07724
  Attn: Frank Reder, Frequency Control Div

Motorola, Incorporated
Solid-State Electronics Department
8201 East McDowell Road
Phoenix, Arizona   85008
  Attn: Norman Dye

34

DISTRIBUTION (Continued)

Sperry Rand Corporation
Clearwater, Florida   33517
   Attn: R. Duncan

Applied Physics Laboratory
Johns Hopkins University
8621 Georgia Avenue
Silver Spring, Maryland   20910

Internal

Horton, B. M., Technical Director
Ellis, V. H., Col./Sommer, H.
   Apstein, M./Guarino, P. A./Kalmus, H. P.
   Spates, J. E.
Schwenk, C. C./Turner, J., 0021
Chief, Lab 100
Chief, Lab 200
Chief, Lab 300
Chief, Lab 400
Chief, Lab 500
Chief, Lab 600
Chief, Div 700
Chief, Div 800
Chief, Lab 900
Pepper, W. H., 260
Jones, H. S., 250
Mak, T. H., 250   (10 copies)
Reggia, F., 250   (10 copies)
Ramos, E., 240
Rotkin, I./Godfrey, T. B./Bryant, W. T.
Klute, C. H./Kohler, H.W.
Technical Information Office, 010   (5 copies)
Technical Reports Br., 870
HDL Library (5 copies)
Bonnell, R., 040
Willis, B. F., 850

DOCUMENT CONTROL DATA - R & D

(Security classification of title, body of abstract and indexing annotation must be entered when the overall report is classified)

1. ORIGINATING ACTIVITY *(Corporate author)*	2a. REPORT SECURITY CLASSIFICATION
Harry Diamond Laboratories Washington, D. C. 20438	UNCLASSIFIED
	2b. GROUP

3. REPORT TITLE

ELECTRONICALLY TUNABLE MICROWAVE BANDPASS FILTER

4. DESCRIPTIVE NOTES *(Type of report and inclusive dates)*

5. AUTHOR(S) *(First name, middle initial, last name)*

Ting Hei Mak
Frank Reggia

6. REPORT DATE	7a. TOTAL NO. OF PAGES	7b. NO. OF REFS
October 1967	38	11

8a. CONTRACT OR GRANT NO.	9a. ORIGINATOR'S REPORT NUMBER(S)
b. PROJECT NO. DA-1C014501B31A	TR-1359
c. AMCMS Code: 5011.11.85400	9b. OTHER REPORT NO(S) *(Any other numbers that may be assigned this report)*
d. HDL Proj No. 28300	

10. DISTRIBUTION STATEMENT

Distribution of this document is unlimited.

11. SUPPLEMENTARY NOTES	12. SPONSORING MILITARY ACTIVITY
	AMC

13. ABSTRACT

An equivalent circuit of two orthogonal striplines coupled by a ferrite (yttrium iron garnet) sphere is derived, using the scattering matrix method. This derivation shows that a nonreciprocal phase shifter can be represented by gyrator networks. Based on this analysis, a YIG bandpass filter, electronically tunable over a very broad frequency range (4:1), is designed by coupling two broadband 180-deg phase shift circuits with a small single crystal YIG sphere.

This report also reviews some basic principles pertaining to filter considerations, analyzes the filter circuit of two orthogonal striplines coupled by a ferrite sphere, and synthesizes the equivalent filter circuit by a scattering matrix method. These results describe the operation of the filter circuit under various terminal excitations.

DD FORM, NOV 65 **1473** REPLACES DD FORM 1473, 1 JAN 64, WHICH IS OBSOLETE FOR ARMY USE.

14. KEY WORDS	LINK A		LINK B		LINK C	
	ROLE	WT	ROLE	WT	ROLE	WT
Ferrites, Magnetics Microwaves Bandpass Filters						

REMOVAL OF EACH CARD WILL BE NOTED ON INSIDE BACK COVER, AND REMOVED
CARDS WILL BE TREATED AS REQUIRED BY THEIR SECURITY CLASSIFICATION.